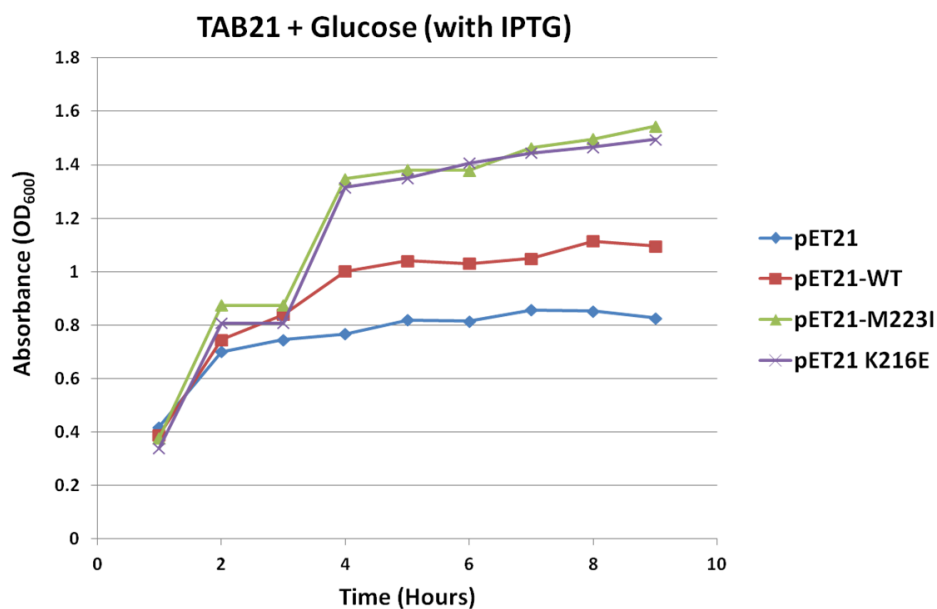
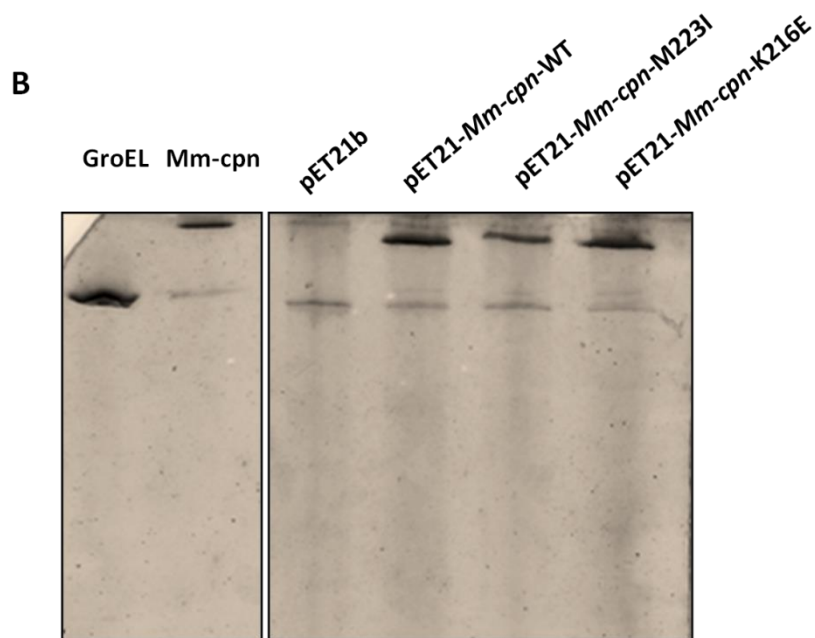
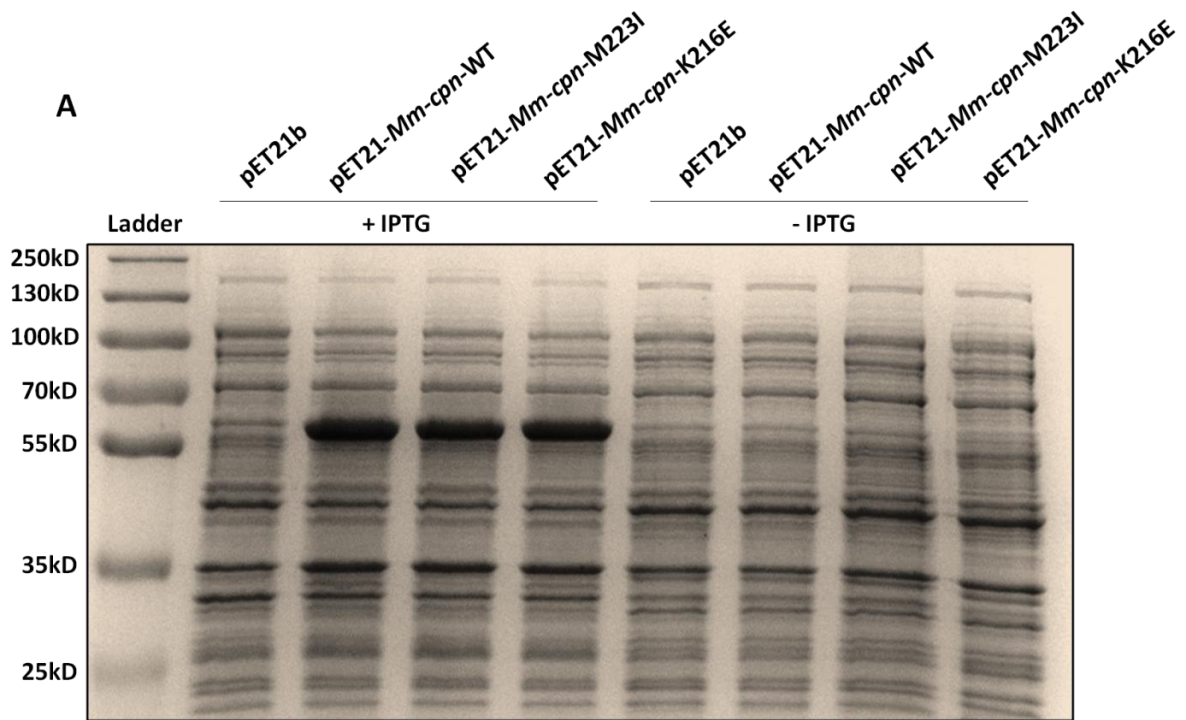


Figure S1**Liquid medium growth analysis of *Mm-cpn* mutants under GroEL depleting conditions**

TAB21 cultures expressing pET21, pET21-*Mm-cpn*, pET21-*Mm-cpn*-M223I and pET21-*Mm-cpn*-K216E were grown overnight in LB containing 0.2% arabinose. They were subsequently diluted into LB containing 0.2% glucose and grown to an OD₆₀₀ of 0.4, at which point 1mM IPTG was added followed by measurement of optical densities over the indicated interval of time. The means of at least three independent experiments are shown.

Figure S2



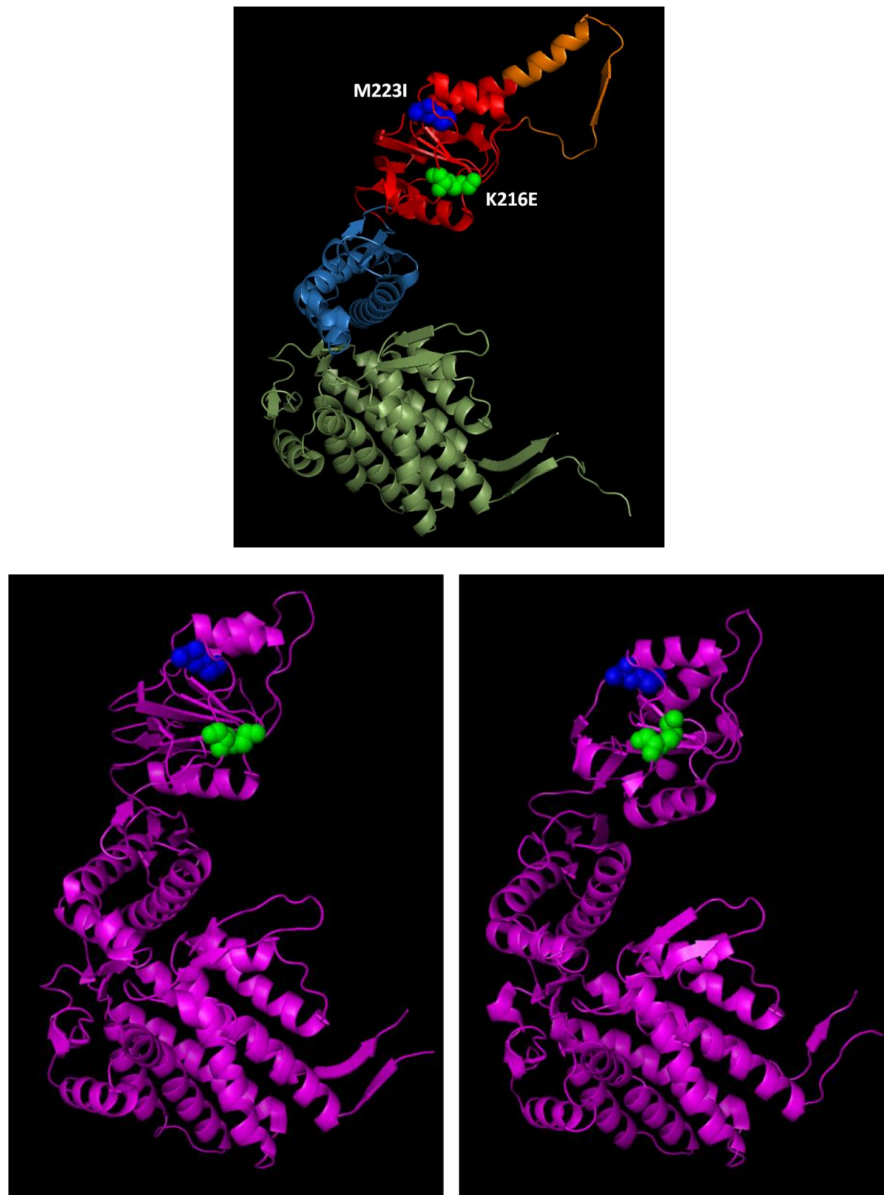
(A) Expression of Mm-cpn-M223I and Mm-cpn-K216E in TAB21

Crude extracts from *E. coli* TAB21 cells containing pET21-*Mm-cpn*, pET21-*Mm-cpn*-M223I and pET21-*Mm-cpn*-K216E either non-induced or induced with 1mM IPTG, analyzed by 10% SDS-PAGE and Coomassie staining.

(B) Assembly of Mm-cpn-M223I and Mm-cpn-K216E in TAB21

Soluble fractions of equal densities of *E. coli* TAB21 cells expressing pET21 empty vector, pET21-*Mm-cpn*, pET21-*Mm-cpn*-M223I and pET21-*Mm-cpn*-K216E in IPTG induced conditions as analyzed by 7.5% Native PAGE and Coomassie staining. Purified Mm-cpn and GroEL proteins were run as controls.

Figure S3 (A)

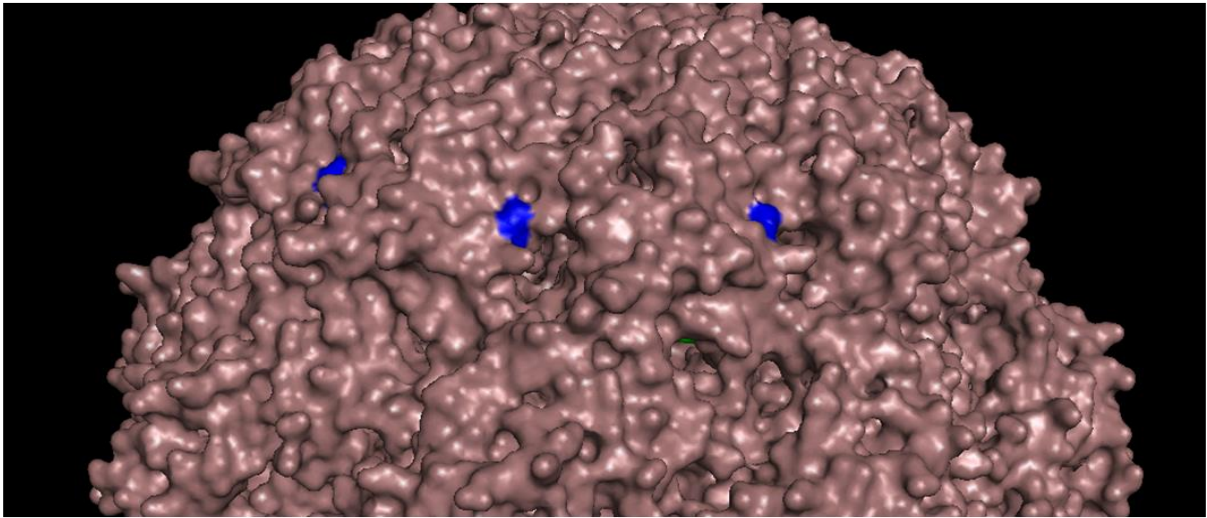


(A) Top : Location of M223 and K216 residues on Mm-cpn subunit.

Mm-cpn subunit showing M223 and K216 residues highlighted in blue and green colour respectively. The subunits were visualized in PyMOL from the PDB structure 3KFK. Red: Apical domain, Blue: Intermediate domain, green: Equatorial domain and Orange: Helical protrusion.

Bottom: Location of M223 and K216 residues on open and closed subunits of Mm-cpn
Mm-cpn subunit showing M223 (blue) and K216 (green) on lidless-closed (left) and lidless-open (right) conformations. The images were derived from PDB codes 3KFB and 3KFE respectively and visualized in PyMOL

Figure S3 (B)

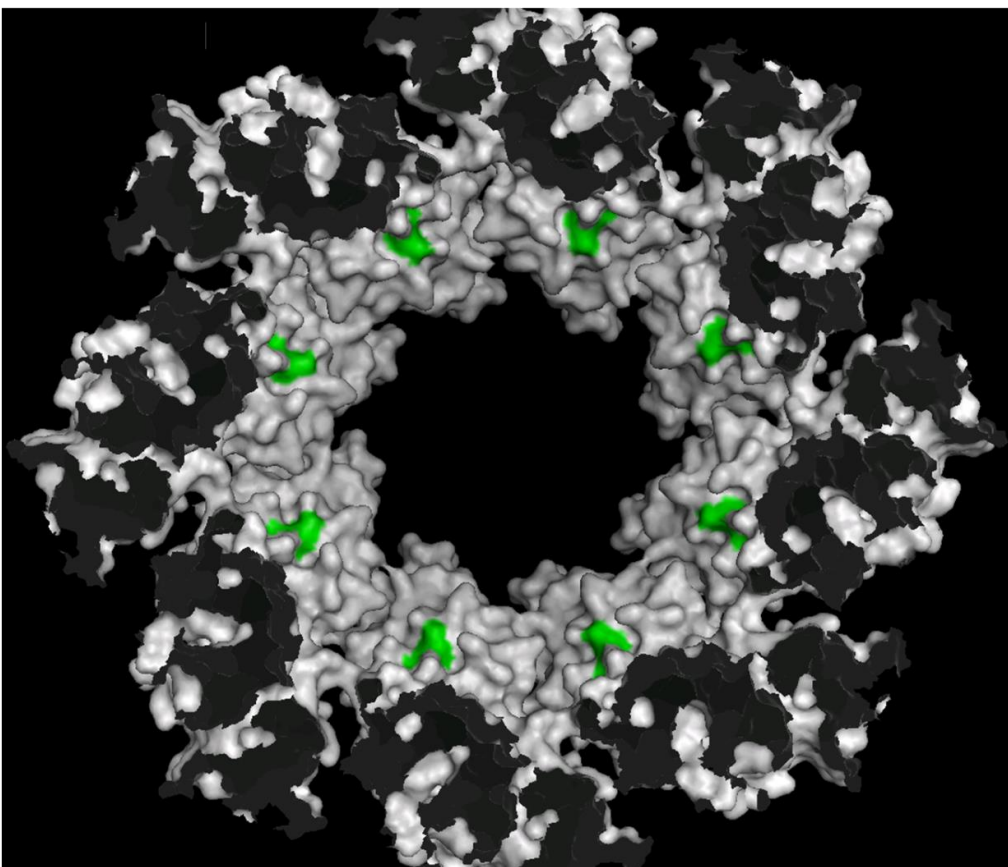
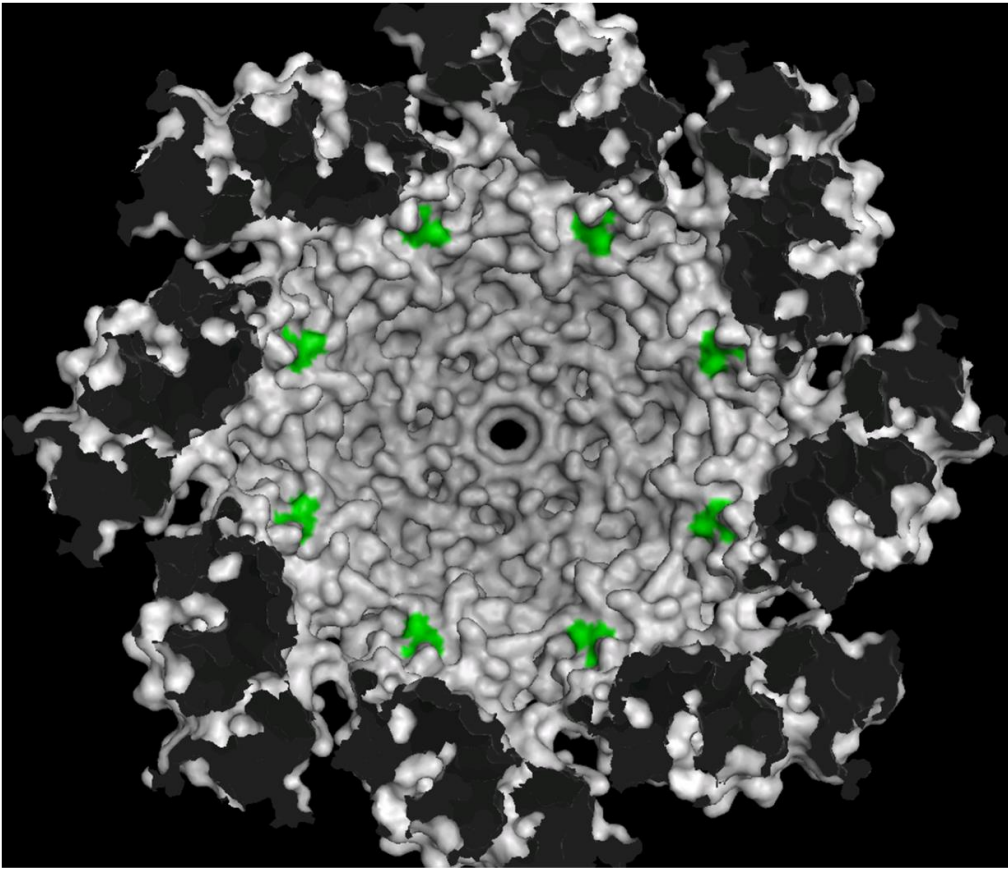


(B) Location of M223 residues on a surface representation of Mm-cpn closed complex

Side view of closed conformation of Mm-cpn complex highlighting M223 residues (blue).

The images were drawn in PyMOL using structures derived from PDB (ID: 3KFK).

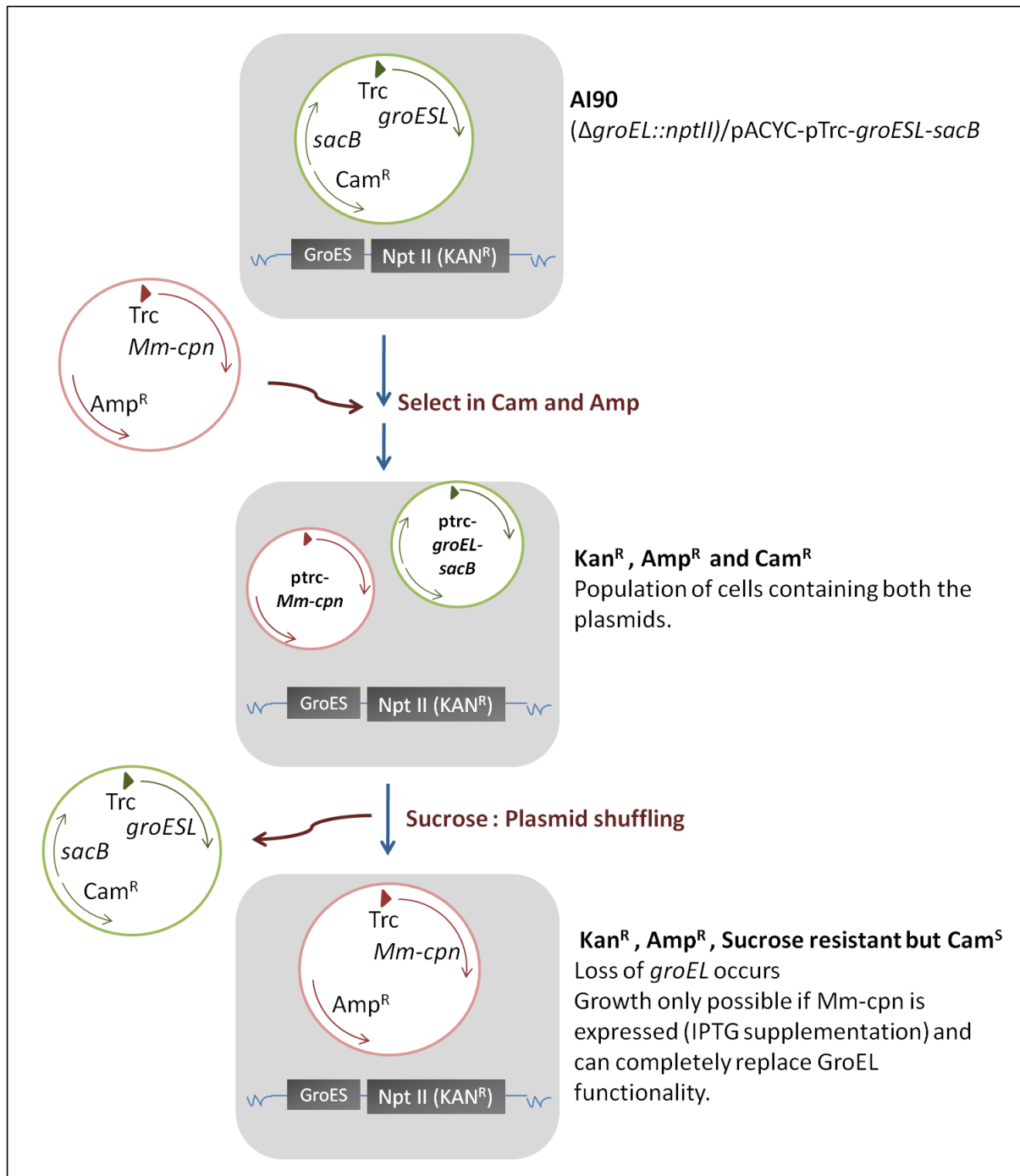
Figure S3 (C)



(C) Location of K216 residues on a surface representation of Mm-cpn closed complex

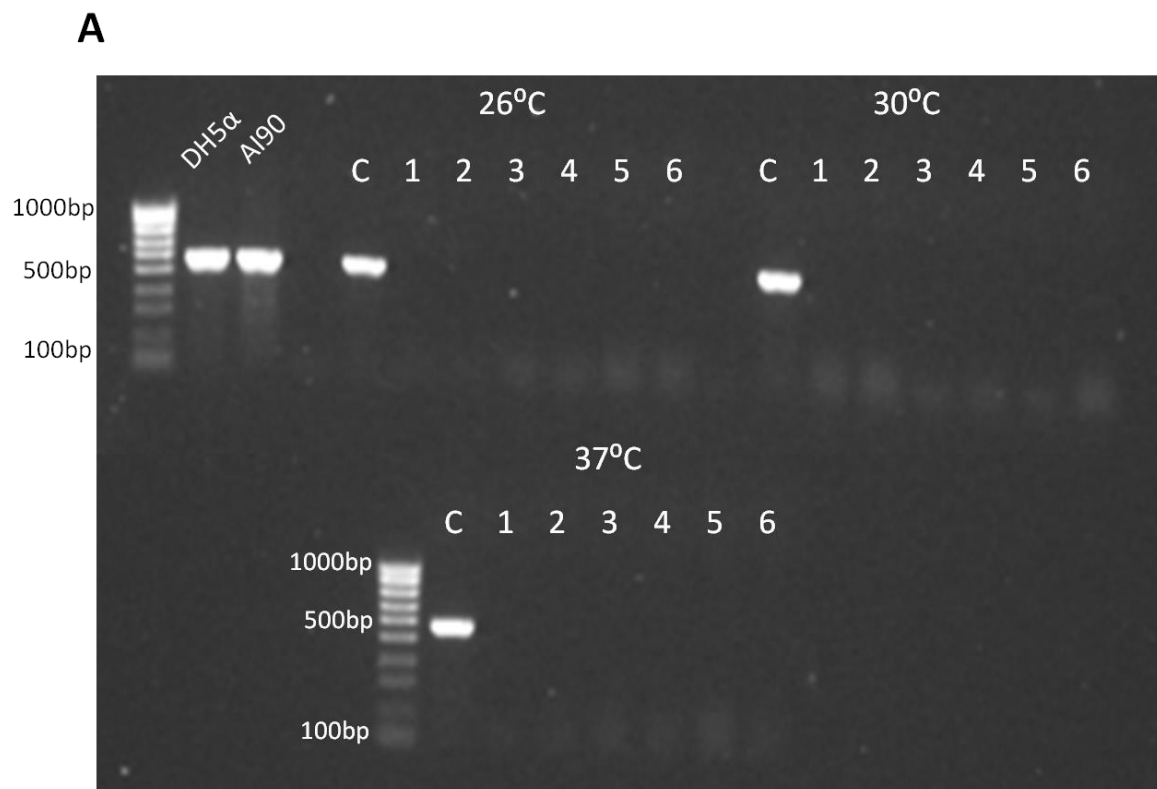
The figure shows the *cis* cavity as viewed from bottom of the cross-sections of closed (above) and open (below) conformations of lidless Mm-cpn complex, highlighting K216 residues (green). The images were drawn in PyMOL using structures derived from PDB (ID: 3KFB and 3KFE).

Figure S4



Plasmid shuffling in *E. coli* to test ability of *Mm-cpn* to complement loss of GroEL.

Figure S5

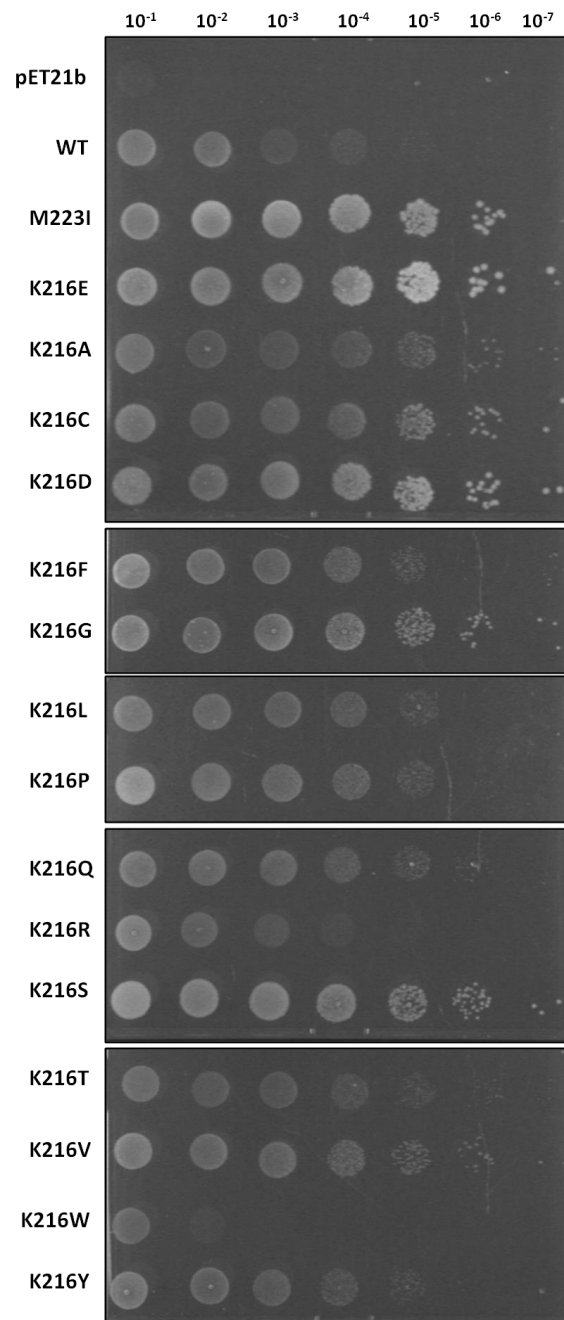


Confirmation of loss of *groEL* gene from AI90 cells with Mm-cpn-K216E

Colony PCR of AI90 cells containing Mm-cpn-K216E using *groEL*-gene internal primers.

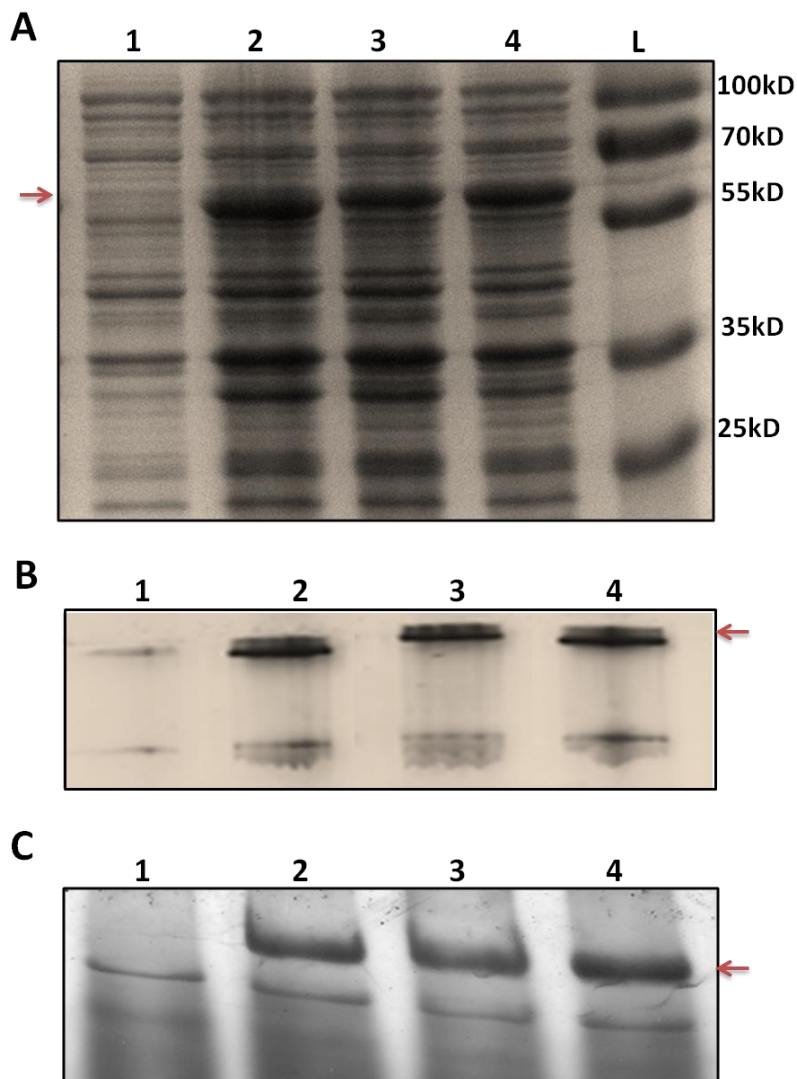
‘C’ denotes positive control (AI90 colonies transformed with *ptrc-groEL*). #1 to #6 denotes six test colonies from plates grown at 25°C, 30°C or 37°C.

Figure S6



Growth of K216n mutants at 30°C under GroEL depleting conditions. TAB21 cells expressing 14 different K216 mutants as indicated under pET21 vector grown on 0.2% glucose and 1 mM IPTG at 30°C for five days.

Figure S7

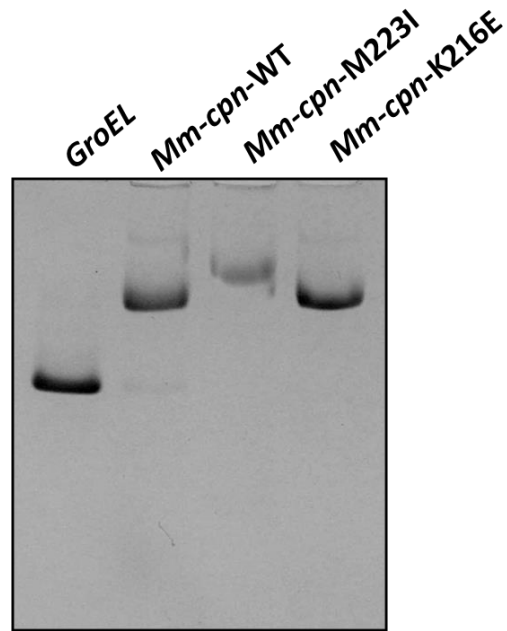


Expression and assembly of D386A mutants in TAB21

(A) Crude extracts of TAB21 cells expressing pET21 empty vector (1), pET21-*Mm-cpn*-D386A (2), pET21- *Mm-cpn* -M223I-D386A (3) and pET21- *Mm-cpn* -K216E-D386A as analysed by 10% SDS PAGE

(B and C) Soluble fractions of the above samples as analyzed by 7.5% Native PAGE (B) and 3-10% Native gradient PAGE (C). All gels stained by Coomassie staining. The arrows indicate the position of the *Mm-cpn* bands.

Figure S8



Native-PAGE analysis of purified Mm-cpn proteins

Purified proteins Mm-cpn-M223I and Mm-cpn-K216E as analysed by Native-PAGE.

Purified GroEL and purified Mm-cpn were used as controls to determine the position of bands on the gels.